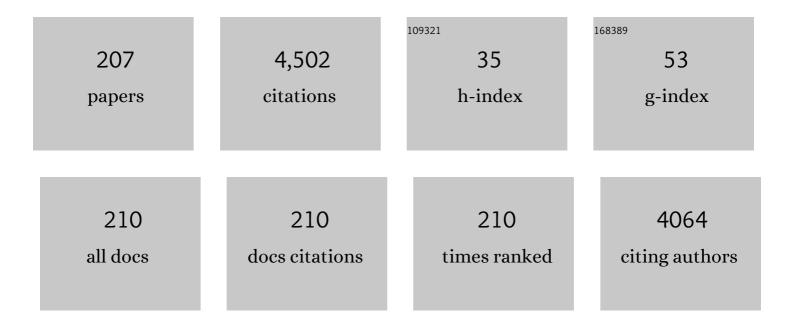
Sergio Valeri

List of Publications by Year in descending order

Source: https://exaly.com/author-pdf/3820280/publications.pdf Version: 2024-02-01



SEDCIO VALEDI

#	Article	IF	CITATIONS
1	Graphene Confers Ultralow Friction on Nanogear Cogs. Small, 2021, 17, 2104487.	10.0	16
2	Structure of Reduced Cerium Oxide Ultrathin Films on Pt(111): Local Atomic Environment and Longâ€Range Order. Advanced Materials Interfaces, 2020, 7, 2000737.	3.7	0
3	Optical and electronic properties of silver nanoparticles embedded in cerium oxide. Journal of Chemical Physics, 2020, 152, 114704.	3.0	12
4	Tribological Properties of High-Speed Uniform Femtosecond Laser Patterning on Stainless Steel. Lubricants, 2019, 7, 83.	2.9	21
5	Highly efficient plasmon-mediated electron injection into cerium oxide from embedded silver nanoparticles. Nanoscale, 2019, 11, 10282-10291.	5.6	27
6	Reducibility of Ag- and Cu-Modified Ultrathin Epitaxial Cerium Oxide Films. Journal of Physical Chemistry C, 2019, 123, 13702-13711.	3.1	6
7	Physical Synthesis and Study of Ag@CaF 2 Core@Shell Nanoparticles: Morphology and Tuning of Optical Properties. Physica Status Solidi (B): Basic Research, 2019, 256, 1800507.	1.5	3
8	Dynamics of the Interaction Between Ceria and Platinum During Redox Processes. Frontiers in Chemistry, 2019, 7, 57.	3.6	11
9	Mesoporous bioactive glasses doped with cerium: Investigation over enzymatic-like mimetic activities and bioactivity. Ceramics International, 2019, 45, 20910-20920.	4.8	19
10	Role of cerium oxide in bioactive glasses during catalytic dissociation of hydrogen peroxide. Physical Chemistry Chemical Physics, 2018, 20, 23507-23514.	2.8	6
11	Cerium-doped bioactive 45S5 glasses: spectroscopic, redox, bioactivity and biocatalytic properties. Journal of Materials Science, 2017, 52, 8845-8857.	3.7	43
12	Contraction, cation oxidation state and size effects in cerium oxide nanoparticles. Nanotechnology, 2017, 28, 495702.	2.6	12
13	Structure of active cerium sites within bioactive glasses. Journal of the American Ceramic Society, 2017, 100, 5086-5095.	3.8	16
14	Cerium Oxide Epitaxial Nanostructures on Pt(111): Growth, Morphology and Structure. Topics in Catalysis, 2017, 60, 513-521.	2.8	9
15	Steering the magnetic properties of Ni/NiO/CoO core-shell nanoparticle films: The role of core-shell interface versus interparticle interactions. Physical Review Materials, 2017, 1, .	2.4	6
16	Tunable spin-wave frequency gap in anisotropy-graded FePt films obtained by ion irradiation. Physical Review B, 2016, 94, .	3.2	1
17	Influence of defect distribution on the reducibility of CeO _{2â^'<i>x</i>} nanoparticles. Nanotechnology, 2016, 27, 425705.	2.6	16
18	Dopant-Induced Diffusion Processes at Metal–Oxide Interfaces Studied for Iron- and Chromium-Doped MgO/Mo(001) Model Systems. Journal of Physical Chemistry C, 2016, 120, 13604-13609.	3.1	14

#	Article	IF	CITATIONS
19	AFM-based tribological study of nanopatterned surfaces: the influence of contact area instabilities. Journal of Physics Condensed Matter, 2016, 28, 134008.	1.8	10
20	Electronic properties of epitaxial cerium oxide films during controlled reduction and oxidation studied by resonant inelastic X-ray scattering. Physical Chemistry Chemical Physics, 2016, 18, 20511-20517.	2.8	24
21	Tribological characteristics of few-layer graphene over Ni grain and interface boundaries. Nanoscale, 2016, 8, 6646-6658.	5.6	28
22	Electrical, optical, and electronic properties of Al:ZnO films in a wide doping range. Journal of Applied Physics, 2015, 118, .	2.5	25
23	Morphology, structural properties and reducibility of size-selected CeO _{2â^'} <i>_x</i> nanoparticle films. Beilstein Journal of Nanotechnology, 2015, 6, 60-67.	2.8	13
24	Electrospun Fibers Containing Bioâ€Based Ricinoleic Acid: Effect of Amount and Distribution of Ricinoleic Acid Unit on Antibacterial Properties. Macromolecular Materials and Engineering, 2015, 300, 1085-1095.	3.6	8
25	Atomic Scale Structure and Reduction of Cerium Oxide at the Interface with Platinum. Advanced Materials Interfaces, 2015, 2, 1500375.	3.7	25
26	Influence of size, shape and core–shell interface on surface plasmon resonance in Ag and Ag@MgO nanoparticle films deposited on Si/SiO x. Beilstein Journal of Nanotechnology, 2015, 6, 404-413.	2.8	17
27	Structure, Morphology and Reducibility of Epitaxial Cerium Oxide Ultrathin Films and Nanostructures. Materials, 2015, 8, 5818-5833.	2.9	29
28	Frictional transition from superlubric islands to pinned monolayers. Nature Nanotechnology, 2015, 10, 714-718.	31.5	33
29	Evidence of Catalase Mimetic Activity in Ce ³⁺ /Ce ⁴⁺ Doped Bioactive Glasses. Journal of Physical Chemistry B, 2015, 119, 4009-4019.	2.6	119
30	Nanoscale frictional behavior of graphene on SiO ₂ and Ni(111) substrates. Nanotechnology, 2015, 26, 055703.	2.6	57
31	ZnO Nanostructure Formation on the Mo(001) Surface. Journal of Physical Chemistry C, 2015, 119, 13743-13749.	3.1	4
32	Structure and Morphology of Silver Nanoparticles on the (111) Surface of Cerium Oxide. Journal of Physical Chemistry C, 2015, 119, 6024-6032.	3.1	29
33	Tunability of exchange bias in Ni@NiO core-shell nanoparticles obtained by sequential layer deposition. Nanotechnology, 2015, 26, 405704.	2.6	22
34	Chromium-Doped MgO Thin Films: Morphology, Electronic Structure, and Segregation Effects. Journal of Physical Chemistry C, 2015, 119, 25469-25475.	3.1	14
35	Structural and morphological modifications of thermally reduced cerium oxide ultrathin epitaxial films on Pt(111). Physical Chemistry Chemical Physics, 2014, 16, 18848-18857.	2.8	46
36	Controlled growth of Ni/NiO core–shell nanoparticles: Structure, morphology and tuning of magnetic properties. Applied Surface Science, 2014, 306, 2-6.	6.1	25

#	Article	IF	CITATIONS
37	Comparing the deposition mechanisms in suspension plasma spray (SPS) and solution precursor plasma spray (SPPS) deposition of yttria-stabilised zirconia (YSZ). Journal of the European Ceramic Society, 2014, 34, 3925-3940.	5.7	61
38	Morphology and Friction Characterization of CVD Grown Graphene on Polycrystalline Nickel. Lecture Notes in Mechanical Engineering, 2014, , 195-204.	0.4	0
39	NiO/Fe(001): Magnetic anisotropy, exchange bias, and interface structure. Journal of Applied Physics, 2013, 113, 234315.	2.5	13
40	Controlled co-deposition of FePt nanoparticles embedded in MgO: a detailed investigation of structure and electronic and magnetic properties. Nanotechnology, 2013, 24, 495703.	2.6	14
41	Structure of Ultrathin CeO ₂ Films on Pt(111) by Polarization-Dependent X-ray Absorption Fine Structure. Journal of Physical Chemistry C, 2013, 117, 1030-1036.	3.1	32
42	Interfacial interaction between cerium oxide and silicon surfaces. Surface Science, 2013, 607, 164-169.	1.9	56
43	Anisotropy-graded magnetic media obtained by ion irradiation of L10 FePt. Acta Materialia, 2013, 61, 4840-4847.	7.9	19
44	Origin of Hydrophobicity in FIB-Nanostructured Si Surfaces. Langmuir, 2013, 29, 5286-5293.	3.5	6
45	Steering the Growth of Metal Adâ€particles via Interface Interactions Between a MgO Thin Film and a Mo Support. Advanced Functional Materials, 2013, 23, 75-80.	14.9	24
46	Orbital anisotropy in paramagnetic manganese oxide nanostripes. Physical Review B, 2013, 87, .	3.2	4
47	Depth-dependent magnetization reversal and spin structure of Fe/NiO exchange-coupled epitaxial bilayers. Applied Physics Letters, 2012, 101, 082412.	3.3	7
48	Assembly and structure of Ni/NiO core–shell nanoparticles. Applied Surface Science, 2012, 260, 13-16.	6.1	15
49	Controlled AFM detachments and movement of nanoparticles: gold clusters on HOPG at different temperatures. Nanotechnology, 2012, 23, 245706.	2.6	11
50	Nature of Ag Islands and Nanoparticles on the CeO ₂ (111) Surface. Journal of Physical Chemistry C, 2012, 116, 1122-1132.	3.1	92
51	Morphology, Stoichiometry, and Interface Structure of CeO ₂ Ultrathin Films on Pt(111). Journal of Physical Chemistry C, 2011, 115, 10718-10726.	3.1	74
52	Assembly and Fine Analysis of Ni/MgO Core/Shell Nanoparticles. Journal of Physical Chemistry C, 2011, 115, 14044-14049.	3.1	17
53	Competition between Polar and Nonpolar Growth of MgO Thin Films on Au(111). Journal of Physical Chemistry C, 2011, 115, 23043-23049.	3.1	36
54	Structure and stability of nickel/nickel oxide core–shell nanoparticles. Journal of Physics Condensed Matter, 2011, 23, 175003.	1.8	35

#	Article	IF	CITATIONS
55	Spontaneous Oxidation of Mg Atoms at Defect Sites in an MgO Surface. Journal of Physical Chemistry C, 2011, 115, 3684-3687.	3.1	12
56	Ag Surface Diffusion and Out-of-Bulk Segregation in CrN-Ag Nano-Composite Coatings. Journal of Nanoscience and Nanotechnology, 2011, 11, 9260-9266.	0.9	6
57	Sliding onset of nanoclusters: a new AFM-based approach. Meccanica, 2011, 46, 597-607.	2.0	1
58	Nanostructured self-lubricating CrN-Ag films deposited by PVD arc discharge and magnetron sputtering. Vacuum, 2011, 85, 1108-1113.	3.5	43
59	Growth and morphology of metal particles on MgO/Mo(001): A comparative STM and diffraction study. Physical Review B, 2011, 83, .	3.2	20
60	Interfacial magnetic structure in Fe/NiO(001). Physical Review B, 2011, 83, .	3.2	9
61	Role of Roughness Parameters on the Tribology of Randomly Nano-Textured Silicon Surface. Journal of Nanoscience and Nanotechnology, 2011, 11, 9244-9250.	0.9	13
62	Secondary electron yield enhancement by MgO capping layers. Surface Science, 2010, 604, 181-185.	1.9	2
63	Depth-dependent magnetic characterization of Fe films on NiO(001). Nuclear Instruments & Methods in Physics Research B, 2010, 268, 361-364.	1.4	6
64	FIB assisted study of plasma sprayed splat–substrate interfaces: NiAl–stainless steel and alumina–NiAl combinations. Surface and Coatings Technology, 2010, 205, 363-371.	4.8	33
65	Hydrophobic effect of surface patterning on Si surface. Wear, 2010, 268, 488-492.	3.1	19
66	Morphology and magnetic properties of size-selected Ni nanoparticle films. Journal of Applied Physics, 2010, 107, .	2.5	31
67	Magnetic couplings and exchange bias in Fe/NiO epitaxial layers. Physical Review B, 2010, 81, .	3.2	24
68	Morphology-induced magnetic phase transitions in Fe deposits on MgO films investigated with XMCD and STM. Physical Review B, 2009, 79, .	3.2	28
69	Image charge screening: A new approach to enhance magnetic ordering temperatures in ultrathin correlated oxide films. Physical Review B, 2009, 79, .	3.2	30
70	Controlling single cluster dynamics at the nanoscale. Applied Physics Letters, 2009, 95, 143121.	3.3	25
71	The analytical relations between particles and probe trajectories in atomic force microscope nanomanipulation. Nanotechnology, 2009, 20, 115706.	2.6	33
72	Fe self-organization on stepped MgO surfaces. Superlattices and Microstructures, 2009, 46, 153-158.	3.1	5

#	Article	IF	CITATIONS
73	Thermally Sprayed Coatings as Interlayers for DLC-Based Thin Films. Journal of Thermal Spray Technology, 2009, 18, 231-242.	3.1	6
74	Increasing nanohardness and reducing friction of nitride steel by laser surface texturing. Tribology International, 2009, 42, 699-705.	5.9	87
75	Fe/NiO(100) and Fe/MgO(100) interfaces studied by X-ray absorption spectroscopy and non-linear Kerr effect. Superlattices and Microstructures, 2009, 46, 107-113.	3.1	11
76	Growth of oxide-metal interfaces by atomic oxygen: Monolayer of NiO(001) on Ag(001). Physical Review B, 2009, 79, .	3.2	33
77	X-ray Photoemission Study of the Charge State of Au Nanoparticles on Thin MgO/Fe(001) Films. Journal of Physical Chemistry C, 2009, 113, 19957-19965.	3.1	27
78	AFM investigation of tribological properties of nano-patterned silicon surface. Wear, 2008, 265, 577-582.	3.1	80
79	Tribological effects of surface texturing on nitriding steel for high-performance engine applications. Wear, 2008, 265, 1046-1051.	3.1	249
80	AFM nanoindentation: tip shape and tip radius of curvature effect on the hardness measurement. Journal of Physics Condensed Matter, 2008, 20, 474208.	1.8	46
81	Morphology evolution and magnetic properties improvement in FePt epitaxial films by in situ annealing after growth. Journal of Applied Physics, 2008, 103, 043912.	2.5	38
82	Local modifications of magnetism and structure in FePt (001) epitaxial thin films by focused ion beam: Two-dimensional perpendicular patterns. Journal of Applied Physics, 2008, 104, 053907.	2.5	15
83	Adhesion detachment and movement of gold nanoclusters induced by dynamic atomic force microscopy. Journal of Physics Condensed Matter, 2008, 20, 354011.	1.8	10
84	Structure and morphology of thin MgO films on Mo(001). Physical Review B, 2008, 78, .	3.2	65
85	Self-organized growth of Ni nanoparticles on a cobalt-oxide thin film induced by a buried misfit dislocation network. Physical Review B, 2008, 77, .	3.2	28
86	Growth and study of Ni nanoparticles films deposited on inert subtrates. Journal of Physics: Conference Series, 2008, 100, 072046.	0.4	1
87	Controlled manipulation of thiol-functionalised gold nanoparticles on Si (100) by dynamic force microscopy. Journal of Physics: Conference Series, 2008, 100, 052008.	0.4	1
88	Effect of the indentation depth on the evaluation of mechanical properties of thin films. International Journal of Materials Research, 2008, 99, 847-851.	0.3	4
89	Metals on oxides: structure, morphology and interface chemistry. Journal of Physics Condensed Matter, 2007, 19, 225002.	1.8	8
90	Hydrolysis at <mml:math <br="" xmlns:mml="http://www.w3.org/1998/Math/MathML">display="inline"><mml:mrow><mml:mi mathvariant="normal">Mg</mml:mi><mml:mi mathvariant="normal">O<mml:mo>(</mml:mo><mml:mn>100</mml:mn><mml:mo>)</mml:mo> mathvariant="normal">Ag<mml:mo>(</mml:mo><mml:mn>100</mml:mn><mml:mo>)</mml:mo> interfaces studied by<mml:math <="" td="" xmlns:mml="http://www.w3.org/1998/Math/MathMI"><td>mml;mo>â^ <td>•< v></td></td></mml:math></mml:mi </mml:mrow></mml:math>	mml;mo>â^ <td>•< v></td>	•< v>

interfaces studied by<mml:math xmlns:mml="http://www.w3.org/1998/Math/MathML" display="inline"><mml:mrow><mml:mi mathvariant="normal. Physical Review B, 2007, 76, .

#	Article	IF	CITATIONS
91	Effects of structural nonplanarity on the magnetoresistance of Permalloy circular rings. Journal of Applied Physics, 2007, 101, 043901.	2.5	2
92	Nanoindentation shape effect: experiments, simulations and modelling. Journal of Physics Condensed Matter, 2007, 19, 395002.	1.8	23
93	Deformation and Adhesion of Elastomer Poly(dimethylsiloxane) Colloidal AFM Probes. Langmuir, 2007, 23, 9293-9302.	3.5	33
94	Nano-structuration of CoO film by misfit dislocations. Surface Science, 2007, 601, 2651-2655.	1.9	32
95	Preparation and characterization of MgO stepped surfaces. Surface Science, 2007, 601, 2636-2640.	1.9	15
96	Structure and electronic properties of Fe nanostructures on MgO(001). Surface Science, 2007, 601, 3902-3906.	1.9	9
97	Ferromagnetic–antiferromagnetic Fe/NiO (100) interface studied by non-linear Kerr effect. Surface Science, 2007, 601, 4362-4365.	1.9	4
98	Magnetic linear dichroism studies of in situ grown NiO thin films. Journal of Magnetism and Magnetic Materials, 2007, 310, 8-12.	2.3	52
99	Magnetic anisotropy engineering in square magnetic elements. Journal of Magnetism and Magnetic Materials, 2007, 316, 106-109.	2.3	4
100	Grain size reduction and magnetic properties improvement by in situ annealing of FePt epitaxial thin films. Journal of Magnetism and Magnetic Materials, 2007, 316, e158-e161.	2.3	12
101	Magnetoresistance of single Permalloy circular rings. Journal of Magnetism and Magnetic Materials, 2007, 316, e944-e947.	2.3	1
102	Iron Oxidation, Interfacial Expansion, and Buckling at theFe/NiO(001)Interface. Physical Review Letters, 2006, 96, 106106.	7.8	43
103	Morphology and optical properties of MgO thin films on Mo(001). Chemical Physics Letters, 2006, 430, 330-335.	2.6	83
104	The Fe/NiO interface studied by polarization dependent X-ray absorption spectroscopy. Nuclear Instruments & Methods in Physics Research B, 2006, 246, 131-135.	1.4	5
105	Focused ion beam induced swelling in MgO(001). Surface Science, 2006, 600, 3718-3722.	1.9	11
106	Morphology and chemical activity at the Au/NiO interface. Surface Science, 2006, 600, 4251-4255.	1.9	10
107	Magnetocrystalline and configurational anisotropies in Fe nanostructures. Journal of Magnetism and Magnetic Materials, 2005, 290-291, 183-186.	2.3	5
108	Submicron-scale patterns on ferromagnetic–antiferromagnetic Fe/NiO layers by focused ion beam (FIB) milling. Nuclear Instruments & Methods in Physics Research B, 2005, 230, 512-517.	1.4	7

#	Article	IF	CITATIONS
109	Absence of oxide formation at the Fe/MgO(001) interface. Surface Science, 2005, 583, 191-198.	1.9	48
110	Initial stages of cobalt film growth on MgO(001) surface. Technical Physics Letters, 2005, 31, 494-497.	0.7	7
111	Polar and non-polar domain borders in MgO ultrathin films on Ag(001). Surface Science, 2005, 588, 160-166.	1.9	36
112	Interplay between magnetocrystalline and configurational anisotropies in Fe(001) square nanostructures. Physical Review B, 2005, 72, .	3.2	31
113	MgOâ^•Ag(001)interface structure and STM images from first principles. Physical Review B, 2004, 70, .	3.2	29
114	Evidence for interdot coupling in an array of micrometric Fe dots. Journal of Magnetism and Magnetic Materials, 2004, 272-276, E1373-E1375.	2.3	0
115	NiO and MgO ultrathin films by polarization dependent XAS. Surface Science, 2004, 566-568, 84-88.	1.9	20
116	Morphology of H2O dosed monolayer MgO(001)/Ag(001). Surface Science, 2004, 566-568, 1071-1075.	1.9	15
117	Chemical reactions and interdiffusion at the Fe/NiO(001) interface. Surface Science, 2004, 572, L348-L354.	1.9	27
118	Magnetism and morphology of Ni/Cu(1 0 0) and Ni–Fe–Ni/Cu(1 0 0) ultrathin films. Journal of Magnetism and Magnetic Materials, 2004, 272-276, E801-E802.	2.3	1
119	OK-edge x-ray absorption study of ultrathinNiOepilayers depositedin situonAg(001). Physical Review B, 2004, 70, .	3.2	28
120	Structure and morphology of ultrathin NiO layers on Ag(001). Thin Solid Films, 2003, 428, 195-200.	1.8	41
121	Oxidation–reduction reactions at as-grown Fe/NiO interface. Surface Science, 2003, 532-535, 409-414.	1.9	28
122	Ultrathin nickel oxide films grown on Ag(001): a study by XPS, LEIS and LEED intensity analysis. Surface Science, 2003, 531, 368-374.	1.9	32
123	Oxide/Metal Interface Distance and Epitaxial Strain in theNiO/Ag(001)System. Physical Review Letters, 2003, 91, 046101.	7.8	87
124	Thickness-dependent strain in epitaxial MgO layers on Ag(). Surface Science, 2002, 507-510, 311-317.	1.9	49
125	EPITAXY OF ULTRATHIN CoO FILMS STUDIED BY XPD AND GIXRD. Surface Review and Letters, 2002, 09, 937-941.	1.1	6
126	Growth and structure of Fe on MgO() studied by modulated electron emission. Surface Science, 2002, 498, 193-201.	1.9	27

#	Article	lF	CITATIONS
127	Experimental and theoretical study of the MgO/Ag() interface. Surface Science, 2002, 505, L209-L214.	1.9	48
128	The Co/Si(111) interface formation: a temperature dependent reaction. Surface Science, 2002, 511, 303-311.	1.9	11
129	Fe epitaxial layers on Cu3Au(001): a structural study by primary-beam diffraction modulated electron emission. Surface Science, 2001, 471, 32-42.	1.9	10
130	Diamond-based composite layers as protective coatings for ion beam extraction systems. Journal of Vacuum Science and Technology A: Vacuum, Surfaces and Films, 2001, 19, 2920.	2.1	2
131	Electron back-scattering contribution to the electron emission anisotropy by keV range electron beams. Journal of Electron Spectroscopy and Related Phenomena, 2001, 114-116, 477-482.	1.7	3
132	Pulsed laser ablation of glassy carbon targets for the coating of ion accelerator electrodes. Surface and Coatings Technology, 2001, 139, 87-92.	4.8	5
133	Structure and growth mode of thin Co films on Fe(001): comparison of purely thermal and ion-assisted deposition. Thin Solid Films, 2001, 397, 116-124.	1.8	3
134	Structural study of thin MgO layers on Ag(001) prepared by either MBE or sputter deposition. Thin Solid Films, 2001, 400, 16-21.	1.8	39
135	Growth, structure and epitaxy of ultrathin NiO films on Ag(001). Thin Solid Films, 2001, 400, 139-143.	1.8	27
136	Breakdown of the bi-dimensional symmetry in bct Fe layers by epitaxy on Co(110) surface. Applied Surface Science, 2001, 175-176, 123-128.	6.1	2
137	Imaging of the structure of ultra-thin cobalt silicide films by inelastically backscattered electrons. Applied Surface Science, 2001, 175-176, 83-89.	6.1	7
138	Structural analysis of epitaxial Fe films on Ni(001). Applied Surface Science, 2000, 162-163, 198-207.	6.1	7
139	K2Te photocathode growth: A photoemission study. Journal of Applied Physics, 2000, 87, 543-548.	2.5	24
140	Structural and electronic properties of thin Co films on Fe(001) and Fe(001)-p(1×1)O in the bct-to-hcp transition regime. Surface Science, 2000, 454-456, 671-675.	1.9	4
141	Structural characterisation of Fe layers on Co(112Ì,,0). Surface Science, 2000, 466, 30-40.	1.9	4
142	In-depth structural characterisation of the bct-hcp phase transition in Co epitaxial films. Europhysics Letters, 1999, 45, 501-507.	2.0	19
143	Growth and morphology of Te films on Mo. Thin Solid Films, 1999, 352, 114-118.	1.8	5
144	Structural and compositional stability of Co oxide grown on (001) bct Co. Applied Surface Science, 1999, 150, 13-18.	6.1	19

#	Article	IF	CITATIONS
145	Growth and structure of cobalt oxide on (001) bct cobalt film. Surface Science, 1999, 423, 346-356.	1.9	61
146	Modulated electron emission for structural characterization of buried layers and interfaces. Progress in Surface Science, 1998, 59, 91-101.	8.3	2
147	MODULATED ELECTRON EMISSION. Surface Review and Letters, 1997, 04, 937-945.	1.1	6
148	MODULATED ELECTRON EMISSION BY SCATTERING-INTERFERENCE OF PRIMARY ELECTRONS. Surface Review and Letters, 1997, 04, 141-160.	1.1	47
149	Development, operation and analysis of bialkali antimonide photocathodes for high-brightness photo-injectors. Nuclear Instruments and Methods in Physics Research, Section A: Accelerators, Spectrometers, Detectors and Associated Equipment, 1997, 385, 385-390.	1.6	25
150	Characterization of Cs2Te photoemissive film: formation, spectral responses and pollution. Nuclear Instruments and Methods in Physics Research, Section A: Accelerators, Spectrometers, Detectors and Associated Equipment, 1997, 393, 464-468.	1.6	17
151	Particle-induced Auger emission from Si monolayers. Surface Science, 1996, 352-354, 719-723.	1.9	0
152	Auger emission by impact of energetic atoms on Si monolayer(s). Surface Science, 1996, 365, 517-524.	1.9	1
153	Auger lineshape modulation by scattering-interference of primary electrons. Journal of Electron Spectroscopy and Related Phenomena, 1995, 72, 299-303.	1.7	3
154	Element-specific, surface and subsurface structural analysis by scattering-interference of primary electrons. Journal of Electron Spectroscopy and Related Phenomena, 1995, 76, 723-728.	1.7	9
155	Scattering interference of energetic electrons along atomic chains: The effect of the atomic environment. Physical Review B, 1995, 52, 14048-14057.	3.2	6
156	Substrate amorphization induced by the sputter deposition process: Geometrical aspects. Journal of Vacuum Science and Technology A: Vacuum, Surfaces and Films, 1995, 13, 394-399.	2.1	6
157	Surface-shift low-energy photoelectron diffraction: Clean and hydrogenated GaAs(110) surface-structure relaxation. Physical Review B, 1995, 51, 2399-2405.	3.2	24
158	Surface sensitivity of ion-induced Auger electron emission (IAE) spectroscopy. Surface Science, 1995, 331-333, 1256-1261.	1.9	3
159	Focusing and defocusing in electron scattering along atomic chains. Physical Review B, 1994, 50, 14617-14620.	3.2	10
160	Angular anisotropy of electron-excited secondary electron emission. Surface Science, 1994, 311, 422-432.	1.9	18
161	Interlaboratory tests of a composite reference sample to calibrate Auger electron spectrometers in the differential mode. Journal of Electron Spectroscopy and Related Phenomena, 1993, 61, 173-182.	1.7	4
162	Diffraction effects in Auger quantitative analysis on III–V compounds. Applied Surface Science, 1993, 70-71, 20-23.	6.1	9

#	Article	IF	CITATIONS
163	Auger electron emission by ion impact on solid surfaces. Surface Science Reports, 1993, 17, 85-150.	7.2	73
164	Ion bombardment influence on the Cr Auger autoionization structure. Solid State Communications, 1993, 86, 695-698.	1.9	2
165	Effect of the incidence geometry on the ion induced Ni-silicides surface compositional modifications. Nuclear Instruments & Methods in Physics Research B, 1993, 80-81, 877-880.	1.4	1
166	Auger electron spectroscopy for structural studies. Rivista Del Nuovo Cimento, 1993, 16, 1-73.	5.7	9
167	PLVV Auger lineshape modulation by incident beam diffraction in InP. Surface Science, 1993, 289, L617-L621.	1.9	6
168	lon Beam-Stimulated Auger Electron Emission from Cr and Cr-Silicides. Physica Scripta, 1992, T41, 246-250.	2.5	7
169	Crystalline effects on Auger and photoelectron emission from clean and Cs-covered GaAs(110) surfaces. Applied Surface Science, 1992, 56-58, 205-210.	6.1	3
170	Alkali metals adsorption kinetics on sputtered and cleaved GaAs(110) surfaces. Surface Science, 1991, 251-252, 995-999.	1.9	4
171	Auger electron spectroscopy study of cleaved and sputter-etched In0.53Ga0.47As surfaces. Thin Solid Films, 1991, 197, 179-186.	1.8	7
172	Ar+-induced silicon Auger spectra: a probe for the sputter-related collisional and emission processes. Nuclear Instruments & Methods in Physics Research B, 1991, 59-60, 37-40.	1.4	6
173	Ion beam effects on the surface and near-surface composition of TaSi2. Nuclear Instruments & Methods in Physics Research B, 1991, 59-60, 98-101.	1.4	9
174	GaAs and InP surface behaviour under ion bombardment, alkali deposition and oxygen exposure. Vacuum, 1990, 41, 643-646.	3.5	5
175	AES and EELS study of alkali-metal adsorption kinetics on either cleaved or sputtered GaAs and InP (110) surfaces. Surface Science, 1990, 238, 63-74.	1.9	18
176	High energy (~ 107 eV) Si peak in Ar + excited auger emission from silicon and silicides. Surface Science, 1989, 220, 407-418.	1.9	12
177	Electronic and vibrational properties of the K/GaAs system. Surface Science, 1989, 211-212, 659-665.	1.9	8
178	Auger-electron emission induced byAr+impact on silicides. Physical Review B, 1988, 38, 13282-13290.	3.2	13
179	Adsorption of monovalent metals on the GaAs(110) surface. Surface Science, 1987, 189-190, 226-231.	1.9	10
180	Electron energy loss spectroscopic investigation of Cr-L2,3 core levels in Cr and chromium silicides. Solid State Communications, 1987, 61, 5-7.	1.9	7

#	Article	IF	CITATIONS
181	Two hole spectra and valence states in chromium and chromium silicides. Journal of Electron Spectroscopy and Related Phenomena, 1987, 43, 121-130.	1.7	2
182	Local structure of Ni2Si. Journal of Electron Spectroscopy and Related Phenomena, 1987, 42, 287-292.	1.7	1
183	Ar+-beam-induced surface and subsurface modifications in Cr-Si compounds. Nuclear Instruments & Methods in Physics Research B, 1987, 19-20, 97-100.	1.4	3
184	Importance of coulomb correlation in silicide spectra. Surface Science, 1986, 168, 164-170.	1.9	6
185	Electron energy-loss spectroscopy of Ni2Si: Valence collective excitation and structural properties. Surface Science, 1986, 168, 204-211.	1.9	8
186	Correlation and autoionization effects in silicide Auger spectra. Thin Solid Films, 1986, 140, 89-94.	1.8	8
187	Core and valence excitations in Ni2Si. Thin Solid Films, 1986, 140, 99-104.	1.8	1
188	AES and EELS study of ErSi2 and its behaviour under ion bombardment and oxygen exposure. Solid State Communications, 1986, 60, 569-573.	1.9	10
189	Electrical and structural characterization of Nb-Si thin alloy film. Journal of Materials Research, 1986, 1, 327-336.	2.6	25
190	L2,3absorption edges inNi2Si. Physical Review B, 1986, 34, 2875-2877.	3.2	17
191	Auger electron spectroscopy study of the sputtering effect on platinum silicide surfaces. Thin Solid Films, 1985, 130, 315-326.	1.8	6
192	Real-space determination of atomic structure and bond relaxation at theNiSi2-Si(111) interface. Physical Review Letters, 1985, 54, 827-830.	7.8	112
193	X-ray absorption near-edge structure and extended x-ray absorption fine-structure investigation of Pd silicides. Physical Review B, 1985, 32, 612-622.	3.2	31
194	AES study of room temperature oxygen interaction with near noble metal-silicon compound surfaces. Surface Science, 1985, 161, 1-11.	1.9	24
195	Correlation effects in valence-band spectra of nickel silicides. Physical Review B, 1984, 30, 5696-5703.	3.2	47
196	Oxygen chemisorption and oxide formation on Ni silicide surfaces at room temperature. Surface Science, 1984, 145, 371-389.	1.9	26
197	Ion-beam-induced modification of Ni silicides investigated by Auger-electron spectroscopy. Physical Review B, 1983, 28, 4277-4283.	3.2	43
198	Spinâ€polarized photoelectron emission study of AlxGa1â^'xAs alloys grown by molecular beam epitaxy. Journal of Applied Physics, 1982, 53, 4395-4398.	2.5	28

#	Article	IF	CITATIONS
199	Valence photoemission study of temperature dependent reaction products in Ni-Si interfaces and thin films. Solid State Communications, 1982, 43, 199-202.	1.9	19
200	Interlayer water and swelling properties of monoionic montmorillonites. Journal of Colloid and Interface Science, 1981, 84, 301-309.	9.4	46
201	Spin polarized photoemission from molecular beam epitaxy-grown be-doped GaAs. Zeitschrift Für Physik B Condensed Matter and Quanta, 1981, 44, 259-264.	1.9	21
202	The oxygen effect in the growth kinetics of platinum silicides. Journal of Applied Physics, 1981, 52, 6641-6646.	2.5	60
203	Viscous layer at the ice surface. Solid State Communications, 1980, 35, 289-291.	1.9	2
204	Cooling effect on the electron states of Si(III)î—,Pd and Si(III)î—,Pt interfaces. Solid State Communications, 1980, 35, 917-920.	1.9	13
205	Energy band associated with dangling bonds in silicon. Physical Review B, 1980, 22, 1926-1932.	3.2	7
206	Edge dislocation energy level in silicon. Physica Status Solidi A, 1978, 50, K123-K126.	1.7	2
207	Mechanical behaviour at ice-metal interfaces. Philosophical Magazine A: Physics of Condensed Matter, Structure, Defects and Mechanical Properties, 1978, 37, 17-26.	0.6	12